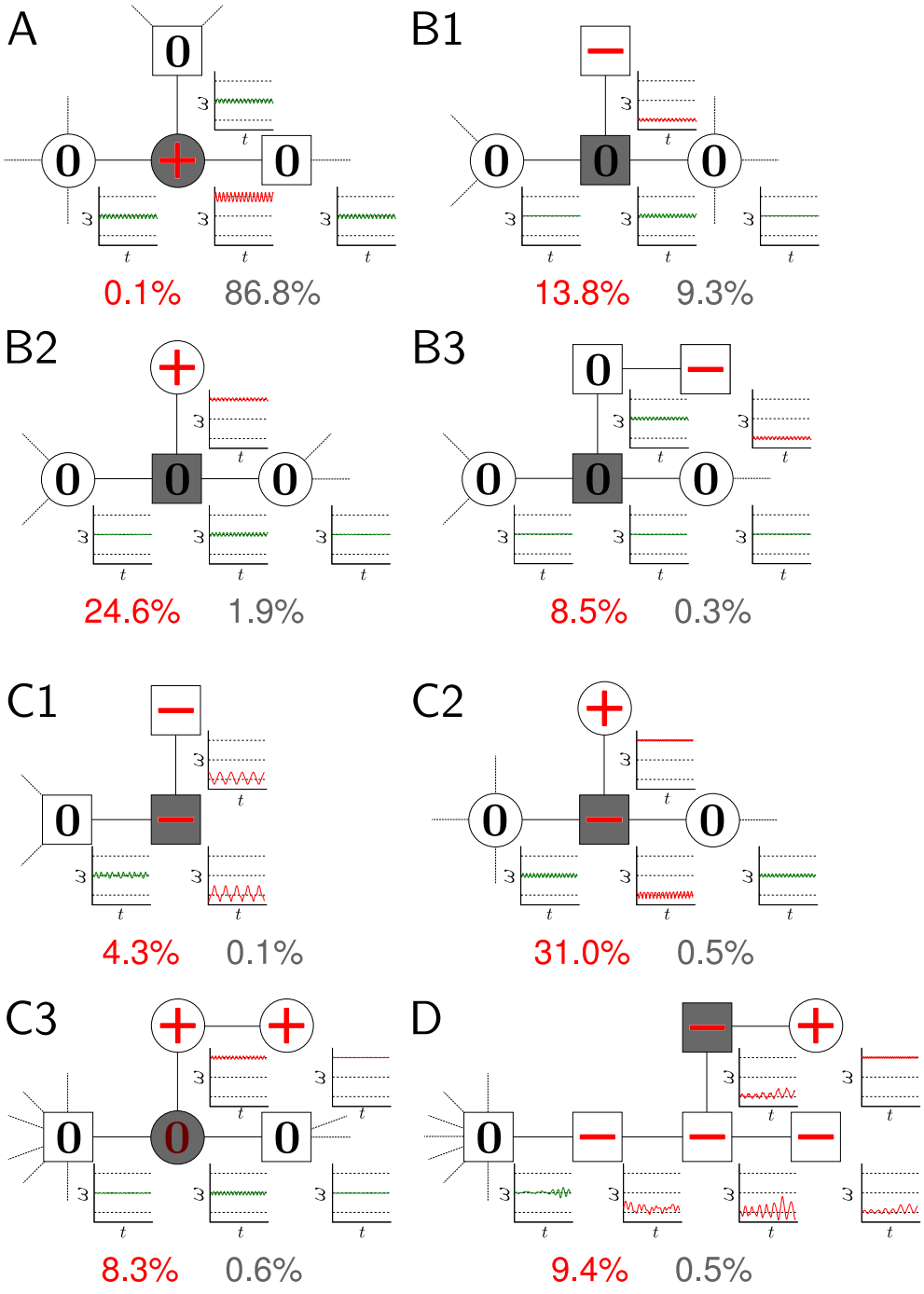

Supplementary Figure 1: **Statistics on non-synchronous states in the power grid ensemble.** Scenarios A, B1-B3, C1-C3 and D show snippets from larger networks consisting of generators (circles) and consumers (squares). The time series indicate a non-synchronous state triggered by a large perturbation hitting the dark grey node. A node marked with $+$, $-$ or 0 has its frequency ω oscillating around $+P/\alpha$, $-P/\alpha$, or 0, respectively. The red (grey) percentage under each scenario gives the share of desynchronizing large perturbations that produce a non-synchronous state like the one shown when hitting nodes with poor (fair) basin stability.

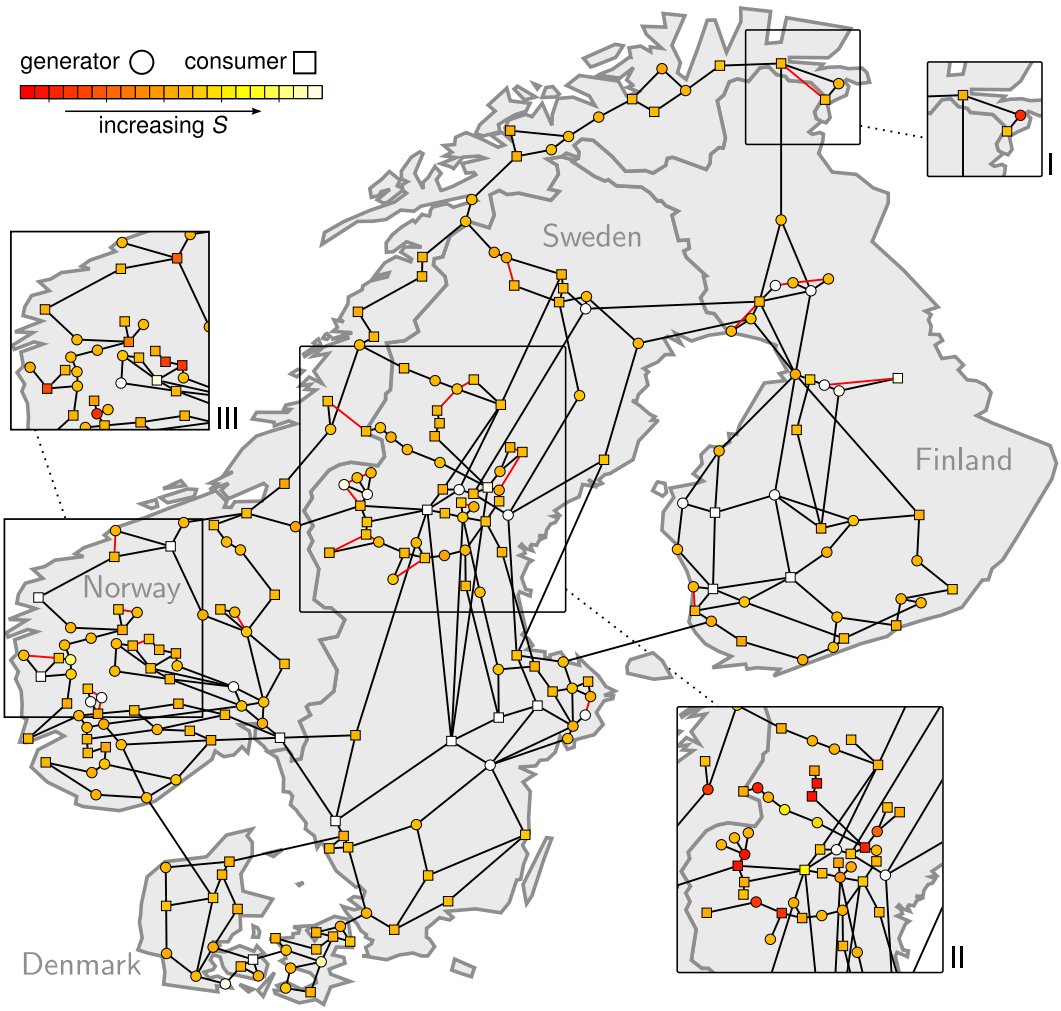

Supplementary Figure 2: **'Healed' Northern European power grid.** Shown is the same grid as in Fig. 4 with $N = 236$ nodes, to whose originally $E = 320$ transmission lines further 27 lines have been added to 'heal' dead trees (see main text). New lines are coloured red. As before, squares (circles) depict $N/2$ net consumers with $P_i = -P$ (net generators with $P_i = +P$). The colour scale indicates how large a node's basin stability S_i is (computed after addition of new transmission lines). Insets I-III show the basin stability values before line addition. Simulation parameters: $\alpha = 0.1$, $P = 1$, and $K = 8$ (see Methods).

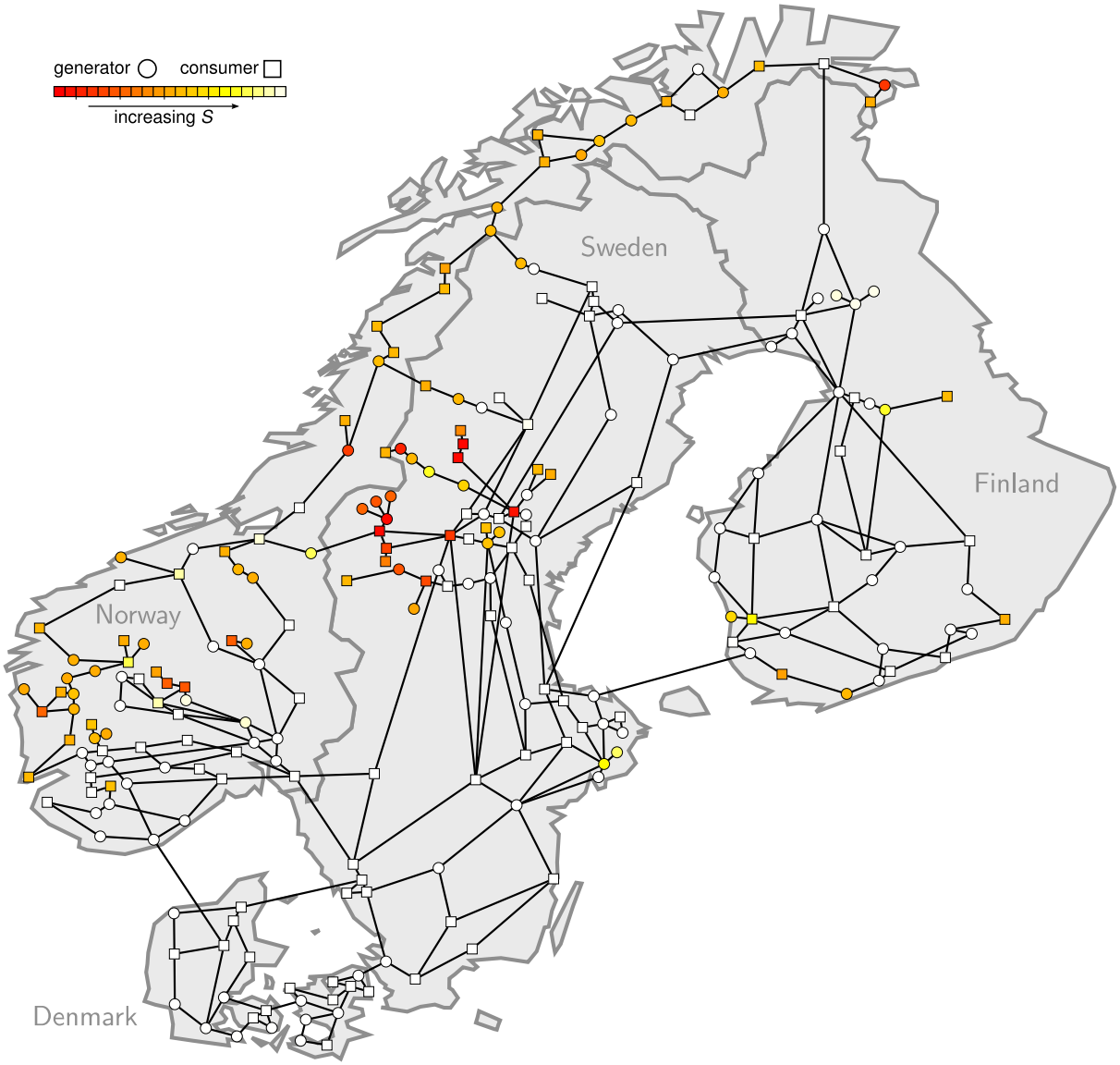

Supplementary Figure 3: **Northern European Power Grid with increased damping.** The grid has $N = 236$ nodes and $E = 320$ transmission lines. The load scenario is, topologically, the same as in Fig. 4, with squares (circles) depicting $N/2$ net consumers with $P_i = -P$ (net generators with $P_i = +P$). The colour scale indicates how large a node's basin stability S_i is. Here, we use different simulation parameters than for Fig. 4: $\alpha = 0.2$ (doubled), $P = 1.6$, and $K = 8$. Whereas in general grid stability increases compared to Fig. 4 (note the many white nodes), nodes adjacent to (or inside of) dead ends or dead trees still typically have significantly lower S_i than non-adjacent nodes.

node i	S_i	S_i^h	node i	S_i	S_i^h	node i	S_i	S_i^h
0	0.57	0.52	30	0.55	0.55	**►60◄**	**0.05**	**0.53**
1	0.53	0.51	31	0.55	0.54	**►61◄**	**0.05**	**0.99**
2	0.52	0.51	32	1.00	1.00	**►62◄**	**0.53**	**0.97**
3	0.51	0.55	33	0.46	0.51	63	0.52	0.54
4	0.53	0.50	**►34◄**	**0.53**	**1.00**	64	0.53	0.54
5	0.53	0.58	35	0.54	0.56	65	0.58	0.57
6	0.54	0.53	36	1.00	1.00	66	0.53	0.53
7	0.53	0.52	37	1.00	1.00	67	1.00	1.00
8	0.54	0.58	38	1.00	1.00	68	0.56	0.53
9	1.00	1.00	39	0.56	0.55	69	1.00	1.00
10	0.49	0.52	40	0.57	0.50	70	0.56	0.52
11	0.54	0.52	41	1.00	1.00	71	0.52	0.56
12	0.97	0.98	42	1.00	1.00	72	0.56	0.56
13	0.53	0.55	43	0.52	0.52	73	0.53	0.57
14	0.56	0.57	44	0.56	0.56	74	0.52	0.53
15	0.92	0.92	45	0.50	0.52	75	0.51	0.54
16	0.51	0.53	46	0.56	0.53	76	0.57	0.55
17	0.52	0.59	47	0.56	0.54	77	0.54	0.54
18	0.53	0.52	48	0.56	0.57	78	0.50	0.50
19	0.55	0.52	49	0.58	0.54	79	0.52	0.54
20	0.53	0.54	50	0.52	0.52	80	0.54	0.53
21	0.53	0.52	51	0.57	0.58	81	0.53	0.55
22	0.51	0.53	52	0.52	0.56	82	0.51	0.49
23	0.51	0.51	53	0.42	0.59	83	0.51	0.51
24	0.55	0.57	54	0.51	0.52	84	0.51	0.52
25	0.58	0.53	55	0.49	0.58	85	0.52	0.54
26	0.59	0.54	56	0.56	0.55	86	0.50	0.53
27	0.53	0.55	**►57◄**	**0.73**	**1.00**	**►87◄**	**0.17**	**0.54**
28	0.55	0.58	58	0.51	0.57	**►88◄**	**0.14**	**0.54**
29	0.57	0.56	59	0.56	0.55	89	0.54	0.58

Supplementary Table 1: **Single-node basin stability of the Northern European power grid.** Listed are the estimated single-node basin stability values for the grid's $N = 236$ nodes in the load scenario pictured in Fig. 4 and detailled in Supplementary Note 4. The column S_i (resp. S_i^h) contains the results before (resp. after) 27 transmission lines are added in order to 'heal' dead ends. This line addition significantly increases (by more than 0.2) the stability of 30 nodes, indicated by ►·◄. At the same time, it significantly decreases (by more than 0.2) the stability of two nodes, indicated by ◄·►.

node i	S_i	S_i^h	node i	S_i	S_i^h	node i	S_i	S_i^h
90	0.50	0.55	120	0.56	0.56	**►150◄**	**0.54**	**1.00**
91	0.55	0.48	121	0.53	0.54	151	0.47	0.55
92	0.51	0.54	**►122◄**	**0.27**	**1.00**	152	0.50	0.56
93	0.53	0.54	123	0.55	0.54	153	0.53	0.53
94	0.54	0.56	124	0.50	0.51	154	0.50	0.53
95	0.55	0.50	125	0.52	0.58	155	0.54	0.54
►96◄	**0.10**	**0.98**	**►126◄**	**0.14**	**0.55**	156	0.52	0.50
►97◄	**0.28**	**0.53**	127	0.49	0.55	157	0.49	0.58
98	0.55	0.52	128	0.57	0.54	158	0.52	0.52
99	0.49	0.54	129	0.55	0.53	159	0.49	0.53
►100◄	**0.05**	**0.51**	130	0.54	0.54	160	0.51	0.53
►101◄	**0.05**	**0.53**	131	0.52	0.55	161	0.56	0.58
102	0.47	0.53	132	0.53	0.53	162	0.50	0.49
103	0.64	0.56	**►133◄**	**0.53**	**1.00**	163	0.51	0.55
104	0.70	0.53	134	0.54	0.54	164	0.54	0.50
105	0.52	0.51	135	0.36	0.50	165	0.53	0.54
►106◄	**0.09**	**0.58**	136	0.55	0.56	166	0.52	0.56
107	0.51	0.54	137	0.55	0.54	167	0.53	0.57
108	0.56	0.56	138	0.52	0.55	168	0.58	0.52
109	0.53	0.54	139	0.55	0.55	169	0.53	0.53
110	0.56	0.54	**►140◄**	**0.56**	**0.86**	170	0.53	0.52
111	1.00	1.00	141	0.52	0.56	171	0.57	0.53
112	0.53	0.54	**►142◄**	**0.22**	**1.00**	172	0.51	0.54
113	0.41	0.52	143	0.51	0.55	**►173◄**	**0.54**	**1.00**
114	0.56	0.53	144	0.56	0.61	174	0.54	0.53
115	0.55	0.58	145	0.52	0.50	**◄175►**	**0.96**	**0.55**
116	0.55	0.48	146	0.54	0.54	**◄176►**	**1.00**	**0.54**
117	0.56	0.54	147	0.56	0.54	177	0.57	0.55
118	0.54	0.48	148	0.53	0.49	178	0.54	0.54
►119◄	**0.14**	**0.57**	**►149◄**	**0.14**	**1.00**	179	0.50	0.55

Supplementary Table 1: **Single-node basin stability of the Northern European power grid (continued).** Listed are the estimated single-node basin stability values for the grid's $N = 236$ nodes in the load scenario pictured in Fig. 4 and detailled in Supplementary Note 4. The column S_i (resp. S_i^h) contains the results before (resp. after) 27 transmission lines are added in order to 'heal' dead ends. This line addition significantly increases (by more than 0.2) the stability of 30 nodes, indicated by ►·◄. At the same time, it significantly decreases (by more than 0.2) the stability of two nodes, indicated by ◄·►.

node i	S_i	S_i^h	node i	S_i	S_i^h
►180◄	**0.18**	**0.52**	210	0.54	0.53
►181◄	**0.16**	**0.51**	211	0.55	0.55
182	0.57	0.57	212	1.00	1.00
►183◄	**0.27**	**0.54**	213	0.54	0.57
184	0.47	0.57	214	0.55	0.52
185	0.52	0.55	215	0.55	0.52
186	0.55	0.50	216	0.54	0.58
►187◄	**0.57**	**0.99**	217	0.54	0.54
188	0.53	0.55	218	0.55	0.55
189	0.56	0.55	219	0.55	0.53
190	0.54	0.55	220	0.53	0.55
191	0.52	0.54	221	0.52	0.51
►192◄	**0.12**	**0.53**	222	0.55	0.48
193	0.56	0.55	223	0.55	0.50
194	0.55	0.58	224	0.55	0.52
195	0.52	0.53	225	0.56	0.58
196	0.57	0.54	226	1.00	1.00
197	0.54	0.54	227	0.54	0.55
198	0.55	0.49	228	0.50	0.52
199	0.54	0.52	**►229◄**	**0.47**	**1.00**
200	0.53	0.54	230	0.53	0.54
201	0.57	0.51	231	0.52	0.53
202	0.56	0.50	232	1.00	1.00
203	0.51	0.56	233	1.00	1.00
204	0.56	0.55	234	0.56	0.52
►205◄	**0.54**	**1.00**	235	0.56	0.51
206	0.56	0.60			
207	1.00	1.00			
►208◄	**0.18**	**0.97**			
►209◄	**0.53**	**0.97**			

Supplementary Table 1: **Single-node basin stability of the Northern European power grid (continued).** Listed are the estimated single-node basin stability values for the grid's $N = 236$ nodes in the load scenario pictured in Fig. 4 and detailled in Supplementary Note 4. The column S_i (resp. S_i^h) contains the results before (resp. after) 27 transmission lines are added in order to 'heal' dead ends. This line addition significantly increases (by more than 0.2) the stability of 30 nodes, indicated by ►·◄. At the same time, it significantly decreases (by more than 0.2) the stability of two nodes, indicated by ◄·►.

Supplementary Note 1

Recall the one-node version of the transient-stability model that reads

$$\dot{\theta} = \omega \tag{1}$$

$$\dot{\omega} = -\alpha\omega + P - \underbrace{K\sin(\theta - \theta_{\text{grid}})}_{=:P_{\text{trans}}} \tag{2}$$

where θ and ω denote phase and angular frequency of the generator's AC voltage vector, measured in a frame of reference that co-rotates with the grid's rated frequency. Hence $\omega = 0$ when the generator is synchronized. The term $-\alpha\omega$ denotes damping, P is the net power input, that is, the sum of locally consumed and locally produced power, and $P_{\text{trans}} = K\sin(\theta - \theta_{\text{grid}})$ quantifies how much power is flowing to the grid across the transmission line whose transfer capacity is $K > 0$. In this version of the model, it is assumed that the grid cannot be influenced by the generator so that $\theta_{\text{grid}} \equiv 0$.

For $K = 0$, this model has a stable non-synchronous limit cycle solution with constant frequency $\omega(t) = P/\alpha =: \Omega$ and phase $\theta(t) = \Omega t + \theta_0$. In numerical simulations we observed that, for a range of K-values larger than zero, a similar stable non-synchronous solution exists which still approximately obeys $\theta_{\text{ns}}(t) \approx \Omega t + \theta_0$. We now derive an expression for the non-synchronous frequency ω_{ns} of this solution. For this purpose, we write $\omega_{\text{ns}} = \Omega + f(t)$ where $f(t)$ is to be determined. Inserting this into Supplementary Equation (2) yields

$$\dot{f} = -\alpha f - K\sin(\Omega t + \theta_0).$$

The specific solution to this equation is

$$f(t) = -\frac{\alpha K}{\Omega^2 + \alpha^2}\left(\sin(\Omega t + \theta_0) - \frac{\Omega}{\alpha}\cos(\Omega t + \theta_0)\right).$$

For $|\Omega|/\alpha = |P|/\alpha^2 \gg 1$, this is approximated by

$$f(t) \approx \frac{K}{\Omega} \cos(\Omega t + \theta_0)$$

and hence

$$\omega_{\mathrm{ns}}(t) \approx \Omega + \frac{K}{\Omega} \cos(\Omega t + \theta_0) \tag{3}$$

as claimed in the main text. Integrating ω_{ns} gives

$$\theta_{\mathrm{ns}}(t) \approx \Omega t + \frac{K}{\Omega^2} \sin(\Omega t + \theta_0) + \theta_0,$$

which means that $\theta(t) \approx \Omega t + \theta_0$ will indeed be observed if $\Omega^2 \gg K$, as is the case for our parameters $|P| = 1, K = 8, \alpha = 0.1$. Supplementary Equation (3) also resembles the observed trajectory quite well if Ω^2 is not that much larger than K.

Supplementary Note 2

In the multi-node model

$$\dot{\theta}_i = \omega_i \tag{4}$$

$$\dot{\omega}_i = -\alpha\omega_i + P_i - \sum_{j=1}^{N} K_{ij}\sin(\theta_i - \theta_j) \tag{5}$$

there exist a multitude of non-synchronous states for the power grids in our ensemble. As $(\sum_i \dot{\omega}_i) = -\alpha(\sum_i \omega_i)$, all of them satisfy

$$\sum_i \omega_i = 0. \tag{6}$$

However, a typical non-synchronous state reached after a large perturbation of the form of Eq. (11) has hit a node with fair basin stability is very different from a typical non-synchronous state reached after a large perturbation has hit a node with poor basin stability (cf. histogram in Fig. 2a). It turns out that this difference has to do with the presence of dead ends. Indeed, it is their proximity that makes poor-stability nodes so unstable.

To see this, we statistically analyze the non-synchronous states that we observed in our ensemble studies. Recall that, to estimate single-node basin stability for a certain node in a grid, we randomly drew $T = 500$ initial states as specified in Eq. (11) and integrated the model equations. From each of these initial states, the grid either converged to synchrony or to a non-synchronous state. The latter outcome emerged quite often, and indeed, when we performed the basin stability estimation procedure for all nodes in all ensemble grids, we encountered a huge number of different non-synchronous states. Yet strikingly, we found that all of them are instances of just eight different representative scenarios.

Classification according to these scenarios relies on the important observation that, in each of the non-synchronous states, the nodes divide themselves into two distinct groups:

The vast majority remain almost synchronous, each having its frequency ω_i oscillating close to zero. However, a few nodes become strongly desynchronized, with ω_i oscillating close to P_i/α, cf. (3). Indeed, P_i/α seems to be the natural frequency of strongly desynchronized nodes.

Now let us look at scenario A in Supplementary Figure 1, which shows four nodes that are part of a larger grid. Two of the nodes are generators ($P_i = +P > 0$, marked by circles) and two are consumers ($P_i = -P$, marked by squares). The time series next to the nodes depict their frequencies in a non-synchronous state that the grid has been pushed into by a large perturbation hitting the dark grey node. Evidently, the dark grey node itself is strongly desynchronized, having ω_i oscillating around P_i/α. In contrast, the three other nodes – and actually all unshown nodes of the grid – remain almost synchronous (with ω_i oscillating around zero). This direct response, in which only the node primarily hit suffers strong desynchronization, is what we take scenario A to represent. This scenario is very important for fair-stability nodes. Indeed, when a random large perturbation hitting a fair-stability node pushes a grid into a non-synchronous state, this state is of type A in 86.8% of the cases. For poor-stability nodes, the corresponding percentage is only 0.1%.

Now let us turn to scenario B1. Again, the corresponding panel in Supplementary Figure 1 shows a non-synchronous state that has been triggered by a large perturbation hitting the dark grey node. As in scenario A, all but one of the nodes remain almost synchronous. However, this time there is an indirect response: Not the primarily hit (dark grey) node, but another secondary node becomes strongly desynchronized. We take scenario B1 to represent states in which the strongly desynchronized secondary node is of the same type as the node primarily hit (both are consumers in the picture) and forms a dead end directly neighbouring that node. The percentage of desynchronizing large perturbations leading to a B1-type non-synchronous state is 13.8% for poor-stability nodes and 9.3% for fair-stability nodes.

Scenario B2 is very similar to scenario B1: Again, it is not the primarily hit (dark grey) node, but a secondary node forming a directly adjacent dead end that suffers strong desynchronization. However, this time the primary node is of the opposite type to the secondary node (consumer and generator, in the picture). Scenario B2 is very important for poor-stability nodes: 24.6% of desynchronizing large perturbations hitting such nodes lead to this kind of non-synchronous state. The respective percentage for fair-stability nodes is just 1.9%.

Scenario B3 depicts another indirect type of response, in which the perturbation entails strong desynchronization of a single secondary node that is not a direct neighbour of the (dark grey) primary node but terminates a multi-node dead end adjacent to it. As scenario B2, this scenario is much more important for poor-stability nodes (8.5%) than for fair-stability nodes (0.3%).

Whereas the indirect scenarios B1-B3 all have one strongly desynchronized node, the indirect scenarios C1-C3 involve two strongly desynchronized nodes. Scenario C1 represents non-synchronous states in which the primary node and a neighbouring dead-end node of the same type are strongly desynchronized. Scenario C2, the most important scenario for poor-stability nodes, represents non-synchronous states in which the primary node and a neighbouring dead-end node of unlike type are strongly desynchronized. The respective percentages for this scenario are 31.0% for poor-stability nodes and 0.5% for fair-stability nodes. Scenario C3 shows a typical non-synchronous state in which the primary node is not among the two strongly desynchronized nodes. These are located in a an adjacent dead end.

Finally, scenario D represents all non-synchronous states in which more than two nodes are strongly desynchronized. We find that these nodes are always located in dead trees. The respective percentages are 9.4% for poor-stability nodes and 0.5% for fair-stability nodes.

To sum up, 86.8% of large perturbations that hit fair-stability nodes and lead to a non-synchronous state can only strongly desynchronize the node primarily affected (scenario A). In contrast, 99.9% of large perturbations that hit poor-stability nodes and lead to a non-synchronous state involve the strong desynchronization of nodes in a nearby dead end (scenarios B1-3, C1-3, D).

This analysis suggests that poor-stability nodes are so unstable because of the dead trees adjacent to them. Indeed, we find that nodes adjacent to dead trees are much less stable than non-adjacent nodes (Fig. 3b).

Supplementary Note 3

Consider a grid consisting of N nodes and characterize its synchronous state by phases θ_i^s and frequencies $\omega_i = 0$, $i = 1, \ldots, N$. A single-node assessment of linear stability can be performed for node i by measuring the maximum Lyapunov exponent $\Lambda_i(\theta, \omega)$ of the synchronous state that pertains to a small perturbation (θ, ω) which pushes the grid to the perturbed state

$$(\theta_j, \omega_j)(0) = \begin{cases} (\theta, \omega) & \text{if } j = i \\ (\theta_j^s, 0) & \text{otherwise} \end{cases} . \tag{7}$$

The magnitude of $\Lambda_i(\theta, \omega)$ measures the rate of convergence or divergence after the perturbation.

For each node i of the Northern European power grid, we estimated $\Lambda_i(\theta_k, \omega_k)$ for $T = 10$ small perturbations (θ_k, ω_k), $k = 1, \ldots, T$, chosen uniformly at random from the box $[-\pi, \pi]^2$ and averaged over them to obtain

$$\bar{\Lambda}_i = \frac{1}{T} \sum_{k=1}^{T} \Lambda_i(\theta_k, \omega_k). \tag{8}$$

Strikingly, we found that, within numerical accuracy, $\bar{\Lambda}_i = -0.05$ for all i. Moreover, we obtained the same outcome for every node in a randomly picked sample of grids from the ensemble.

Why is that? A quick explanation can be deduced from the analysis of Motter et al., who reported[16] that a grid's synchronous state $(\theta_i^s, \omega_i^s = 0)$ is linearly stable if each of the

Lyapunov exponents

$$\Lambda_{\pm}^{j} = -\frac{\alpha}{2} \pm \mathrm{Re}\left[\frac{1}{2}\sqrt{\alpha^2 - 4g_j}\right], \;\; j = 2, \ldots, N \tag{9}$$

is negative. Therein,

$$0 = g_1 < g_2 \leq \ldots \leq g_N \tag{10}$$

denote the eigenvalues of the matrix

$$G_{ij} = \begin{cases} -K_{ij}\cos(\theta_i^s - \theta_j^s) & \text{if } i \neq j \\ -\sum_{k \neq i} G_{ki} & \text{otherwise} \end{cases} \tag{11}$$

For the Northern European grid and every ensemble grid, we found that the product $4g_j$ is of the order of 1 for every $j \in \{2, \ldots, N\}$ whereas $\alpha^2 = 0.01$ at our parameter settings. This means that the square-root term in Supplementary Equation (9) is purely imaginary and $\Lambda_{\pm}^{j} = -\alpha/2$ for every $j \in \{2, \ldots, N\}$. In other words: All non-zero Lyapunov exponents are the same and equal to $-\alpha/2 = -0.05$ at our settings, in perfect agreement with our numerical findings.

Supplementary Note 4

For the sake of reproducability, we here supply some network data on the Northern European power grid. It has $N = 236$ nodes and $E = 320$ edges. Its edge list is given by

0-1	1-2	2-3	3-4	4-5	5-6	6-7	7-0	7-40	0-8	8-5	8-3
2-9	9-10	10-11	11-12	12-3	11-9	8-13	9-14	14-15	15-16	16-17	17-18
18-15	14-19	19-20	20-21	21-15	21-22	22-23	23-24	24-21	23-25	25-26	26-27
27-28	28-29	29-26	29-30	30-31	31-25	28-32	32-30	32-33	33-34	33-35	35-32
33-36	36-32	32-37	37-38	38-36	39-40	40-31	31-39	40-41	41-37	41-42	42-43
43-41	33-44	44-45	45-46	46-44	44-47	47-48	47-223	48-36	33-49	49-44	49-50
50-51	51-38	51-52	52-53	53-54	55-53	53-56	56-57	57-58	58-59	58-60	60-61
61-62	61-63	61-64	53-65	65-66	66-50	48-67	67-68	68-69	69-70	70-57	57-69
69-71	71-72	70-71	71-73	73-74	74-75	75-76	76-77	77-78	78-79	79-80	80-81
81-82	82-83	83-84	84-71	84-112	43-85	85-57	85-90	86-87	87-88	88-89	88-90
90-91	91-92	92-93	93-38	92-65	65-94	94-95	95-96	96-97	97-98	97-99	96-100
100-101	101-102	96-103	103-104	104-105	105-106	106-107	57-37	37-96	53-37	67-108	108-48
108-109	109-110	110-111	111-68	68-96	111-112	112-113	113-110	113-114	113-115	115-67	57-60
60-116	116-117	117-118	118-119	119-120	119-76	117-121	121-122	122-123	122-124	124-125	125-126
126-127	125-128	128-129	129-130	130-131	131-117	122-132	132-133	133-134	134-135	135-136	135-137
135-138	138-139	139-140	140-141	141-142	142-143	142-144	144-140	144-145	145-146	146-147	147-148
148-149	149-150	149-151	148-152	152-153	153-154	154-155	155-156	156-157	157-158	158-159	159-160
160-13	13-161	161-157	161-162	162-163	163-13	163-164	164-165	165-154	165-147	164-166	166-167
167-168	168-42	42-162	42-169	169-170	170-152	162-171	171-153	153-169	168-166	167-125	125-172
172-167	167-173	173-166	166-174	174-173	173-175	175-174	174-176	176-177	177-175	175-178	178-177
179-180	180-181	181-182	182-173	181-175	111-183	183-184	184-185	184-109	184-186	186-187	187-183
187-188	187-189	187-190	190-191	191-192	192-193	191-194	194-195	195-196	196-197	195-198	198-197
197-199	199-200	200-201	201-202	200-203	203-202	202-204	204-81	190-183	183-205	186-183	186-206
206-207	207-208	208-209	208-210	210-211	211-206	210-212	212-186	210-213	213-212	213-214	214-186
214-215	215-216	216-217	217-218	218-219	219-220	220-221	221-222	222-223	223-224	224-225	225-219
225-226	226-227	227-220	227-228	228-217	225-229	229-224	229-226	229-230	229-231	231-232	232-233
233-212	233-229	232-234	234-233	234-186	212-226	226-235	235-213				

The edge list was extracted from a schematic map published by Svenska Kraftnät, the Swedish grid operator, in its 2009 annual report. The randomly drawn load scenario for nodes 0 to 235 on which the results shown in Fig. 4 are based is given by (read from left to right and from top to bottom; for example the nodes labelled 1 to 4 in Fig. 4 correspond to nodes 192, 208, 96, and 142 in this list)

0	0	1	1	1	0	1	0	0	0	1	0	1	1	1	1
1	1	0	0	0	0	0	1	0	1	0	0	0	0	1	0
1	1	1	1	0	0	0	0	0	0	0	0	1	1	0	1
0	0	0	1	1	1	1	0	0	0	0	0	0	1	1	1
1	0	0	1	0	1	0	0	0	1	1	0	1	0	0	0
0	1	1	1	0	1	0	1	0	1	0	1	1	0	0	1
0	1	0	0	0	0	0	1	1	1	1	0	0	1	1	1
0	0	0	1	1	0	0	1	0	1	0	1	1	1	0	1
0	1	1	0	0	0	1	0	0	1	1	1	1	0	0	1
1	0	0	1	0	1	1	0	0	1	0	0	0	1	1	0
1	1	0	1	1	1	1	1	1	0	0	0	0	1	0	0
1	1	0	0	0	0	1	0	1	1	1	1	1	1	1	0
1	0	0	1	0	0	1	1	1	0	0	1	1	1	0	1
1	0	0	0	1	1	0	1	0	1	1	0	1	1	0	1
0	1	0	1	0	0	1	1	1	0	1	1				

where 0 represents a net consumer and 1 a net generator. The following 27 edges are added to the grid in the process of 'healing' dead ends

193-191	205-189	185-183	189-188	209-207	34-45	127-125	136-137	143-141	150-148	151-150	120-107
123-132	102-73	73-72	114-83	62-60	62-64	64-63	89-90	54-55	86-59	98-99	178-179